FRACTURE-MECHANICS-BASED ESTIMATES OF MAGNITUDE OF INDUCED EARTHQUAKES

Martin **GALIS**, Jean-Paul **AMPUERO**, P. Martin **MAI**

KAUST – King Abdullah University of Science and Technology, Thuwal, Saudi Arabia (MG, PMM)
Seismological Laboratory, CalTech – California Institute of Technology, USA (JPA)

martin.galis@kaust.edu.sa
ces.kaust.edu.sa

1 SUMMARY

This work is a first step towards a more complete integration of earthquake physics and rupture dynamics into theoretical and computational frameworks for modeling induced and triggered seismicity.

We present physics-based predictions of the rupture arrest size. We verify our approach against results of 3D dynamic rupture simulations.

Our approach provides estimates that are qualitatively consistent with numerical results and thus provide insight into relations between magnitude, background stress, initial stress and stimulating pressure in generic, yet idealized situations.

2 INTRODUCTION

Galis et al. (2015) investigated conditions for initiating ruptures by localized stresses in 3D and derived theoretical relations between the properties of overstressed nucleation regions (their size, shape and overstress level) and the ability of dynamic ruptures to either stop spontaneously (sub-critical ruptures) or runaway (super-critical ruptures). They found that

- the initiation is mostly controlled by the overstressed area if the aspect ratio of the initiation zone is close to 1
- rupture is confined inside the initiation zone if the initiation area is smaller than estimated by Uenishi (2009)
- stopping ruptures occur if the initiation area is between estimates by Uenishi (2009) and A_2 by Galis et al. (2015)

Figure 1 Illustration of critical area estimated by Uenishi 2009 for high background stress and by estimate A_2 (Galis et al., 2015) for low background stress. Note the good agreement between numerical results and both estimates.

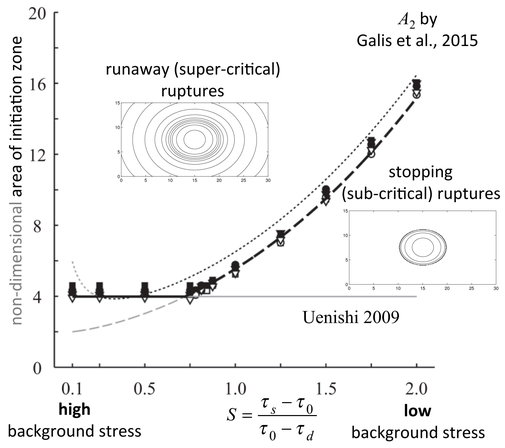

Krammer et al. (2015) used similar approach in 2D to successfully predict the relation between rupture arrest distance and external loading in laboratory experiments in which frictional sliding is nucleated by localized stresses.

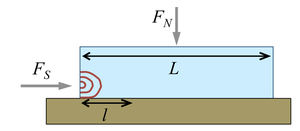

Figure 2 ***above***: sketch of the experiment by Rubinstein et al., 2007 ***right***: comparison of experimental results with theoretical results obtained using Linear Elastic Fracture Mechanics - LEFM (from Krammer et al., 2015)

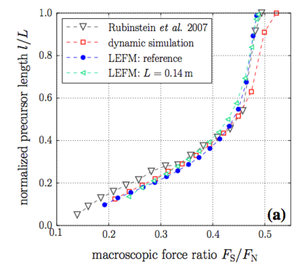

Here we apply and extend these results to situations that are representative for the induced seismicity environment

3 VERIFICATION

I. Assumptions and approximations

- a 3D problem
- crack is at rest if $\eta K_0\left(R,\alpha_1,\alpha_2,\ldots\right) = K_c = \sqrt{2\mu G_c}$, where
  - K_0 is stress intensity factor for tensile mode

$$K_0\left(R,a\right) = \frac{2}{\sqrt{\pi R}} \int_0^R \frac{\Delta\tau\left(r,a\right)}{\sqrt{R^2 - r^2}} r\, dr$$

  - R is radius of crack at arrest
  - $\alpha_1,\alpha_2,\ldots$ are parameters of the nucleation patch (for example, radius of initiation zone, pressure amplitude, time)
  - η is an adjustable factor to account for departures from circularity, the effect of dynamic overshoot, etc.
- the resulting equation for rupture arrest is solved numerically
- working explicitly with stress drop $\Delta\tau$ allows for application of our theory to various cases

II. Verification with numerical simulations

a. Rupture arrest area

Figure 3 illustrates that our theory predicts final rupture area in qualitative agreement with numerical results for various values of the strength parameter, shapes of initiation zone and types of initiation, however, a correction factor is applied to get also quantitative agreement.

b. Conversion of rupture arrest area to M_0

M_0 is computed from rupture arrest area using a scaling relation for a strike-slip event by Mai and Beroza (2000). Resulting M_W is generally 0.2 lower than M_W calculated from final slip from dynamic rupture simulations. Using scaling relations by other authors or for other faulting type may generally lead to variations of ±0.5 magnitude unit.

a) initial traction higher than static traction **b)** low normal traction **c)** normal traction determined by a 2D Gaussian

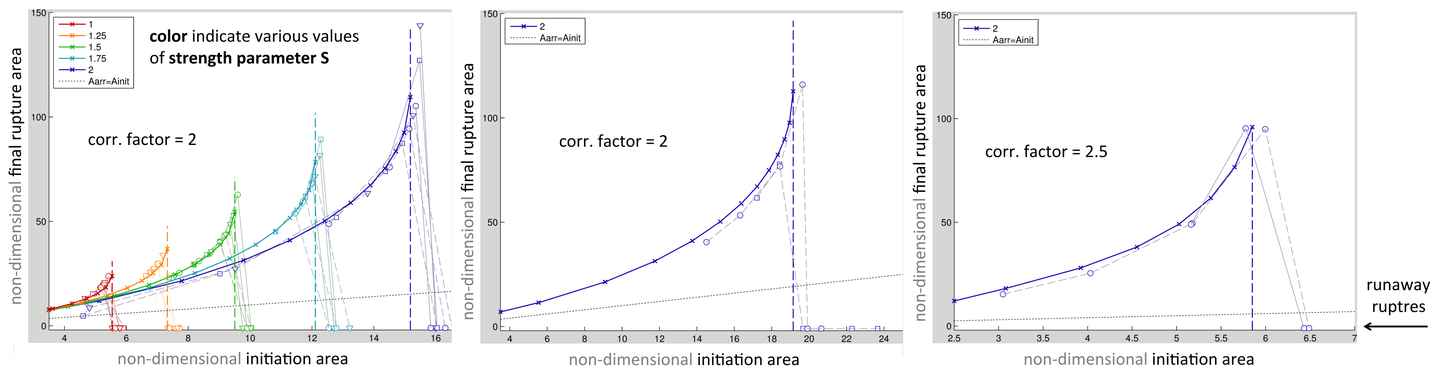

Figure 3 Comparison of rupture arrest area predicted by our approach with final rupture area from numerical simulations for various values of strength parameter S for three types of initiation: **a)** initiation by an overstressed zone with initial traction higher than static traction, **b)** initiation by zone with low normal traction (consequently static traction inside the zone is lower than initial traction), **c)** initiation using lower normal traction that varies smoothly in space following a 2D Gaussian. Circles and gray lines depict numerical results, our predictions are depicted by bold color lines and crosses.

4 ESTIMATES OF FINAL RUPTURE AREA AND MAGNITUDE

I. Pore-pressure solution

- we consider solution of the radial-flow diffusivity equation for cylindrical reservoir with no-flow boundaries and constant flow rate (Lee et al., 2003)
- the solutions is valid for any point inside a cylindrical reservoir during 'infinite-acting' as well as 'pseudosteady-state' stages

II. Parameters for pore-pressure solution

- we adopt parameters of Basel geothermal reservoir (Häring et al., 2008; Dyer et al., 2008; Deichmann & Giardini, 2009)
- stimulation of Basel reservoir was performed with highly increasing flow rates and, naturally, size and permeability of the reservoir changed in response to the stimulation. therefore, we use average parameters to perform a simple parametric study to investigate effects of some parameters on magnitudes of induced events
- we considered:
  - three flow rates, q = 500 l/m, 1500 l/m, 3000 l/m
  - three sizes of reservoir, R = 250 m, 500 m, 750 m

III. Frictional parameters and fault position

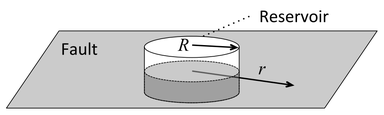

Figure 4 A sketch showing relative position of a fault and a reservoir.

- in order to have radially symmetric stress drop, we consider a fault parallel to the reservoir (Figure 4)
- *Note*: Our choice can be considered as a conservative scenario. A fault crossing the reservoir would be more typical but the pressurized area would be smaller than in our choice.
- frictional parameters are summarized in table:

conf.	shear traction	normal traction	dynamic coef. of fric.	static coef. of fric.	dc	S
A	69.11 MPa	120 MPa	0.525	0.65	0.4 m	1.45
B	69.11 MPa	120 MPa	0.525	0.68	0.4 m	2.0
C	70.56 MPa	120 MPa	0.525	0.68	0.4 m	1.45

IV. Observations / Implications

Configuration A (Figures 5 and 6)

- results summarized in Figure 5 indicate that M_w of the largest stopping rupture only marginally varies with reservoir size and flow rate
- for a fixed flow rate, the size of reservoir does not affect how long it takes to generate a runaway rupture
- results for R = 750 m, indicate that the area of reservoir is fully ruptured before the first stopping ruptures appear outside a reservoir
- comparison of pore-pressure (Figure 6) reveal that conditions for runaway ruptures are much less realistic for small reservoir, which has to be pressurized to ~350MPa, than for large reservoir, which has to be pressurized to ~50MPa

Configuration B (Figure 7)

- comparison of results in Figure 7 with those for configuration A shows that
  - transition to runaway ruptures occurs at much later times than for configuration A
  - M_w of the largest stopping rupture for configuration B is larger than that for configuration A
  - transition to runaway ruptures occurs at even higher pressures (due to longer injection) than for configuration A - ~550 MPa for R = 250m and ~60-90MPa for R = 750m

Configuration C (Figure 8)

- comparison of results in Figure 8 with those for configuration A shows that, although S parameter is the same,
  - maximum M_w before transition to runaway ruptures is systematically lower
  - transition to runaway ruptures occurs sooner and, consequently, at lower pressures than for configuration A – ~300MPa for R = 250m and ~30-60MPa for R = 750m

Comparison of maximum M_w for configuration A

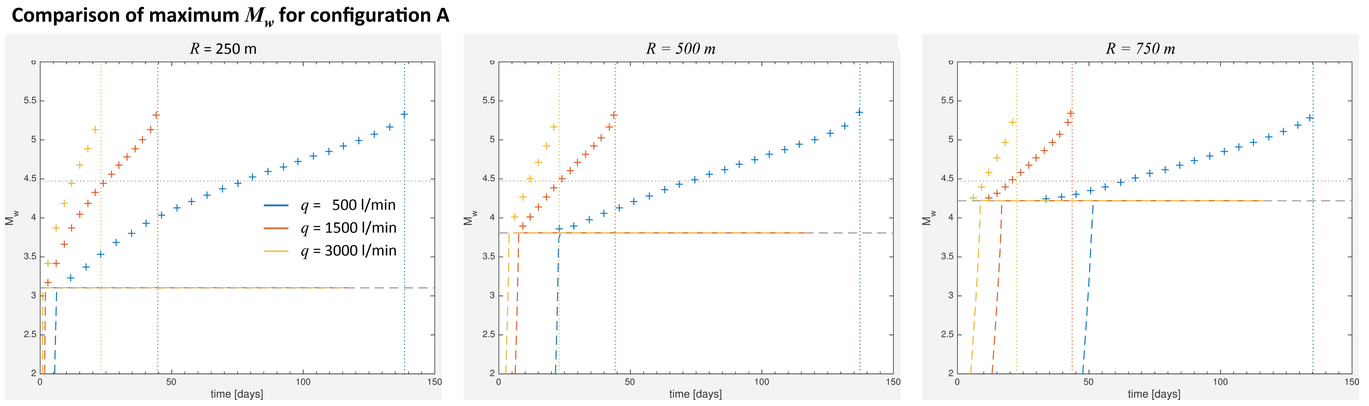

▲ **Figure 5** Comparison of maximum M_w for configuration A as predicted by our approach for three considered sizes of reservoir and three considered flow rates. Vertical dotted lines indicate times of transition from stopping to runaway ruptures. Colored dashed lines indicate M_w corresponding to over critically pressurized area. Horizontal gray dashed line indicate M_w corresponding to area of reservoir. Horizontal dotted line indicate M_w corresponding to the critical area by Uenishi 2009.

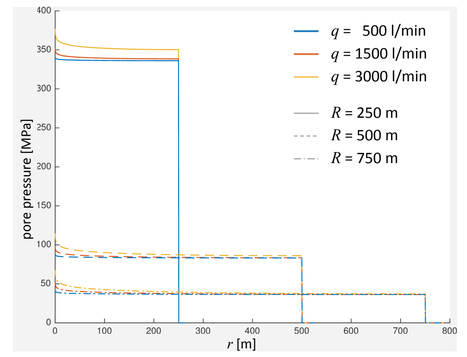

▶ **Figure 6** Comparison of pore pressure in reservoir at the time of transition to runaway ruptures.

▼ **Figure 7, 8** Comparison of maximum M_w for configuration B and C as predicted by our approach. See also Figure 5.

Comparison of maximum M_w for configuration B

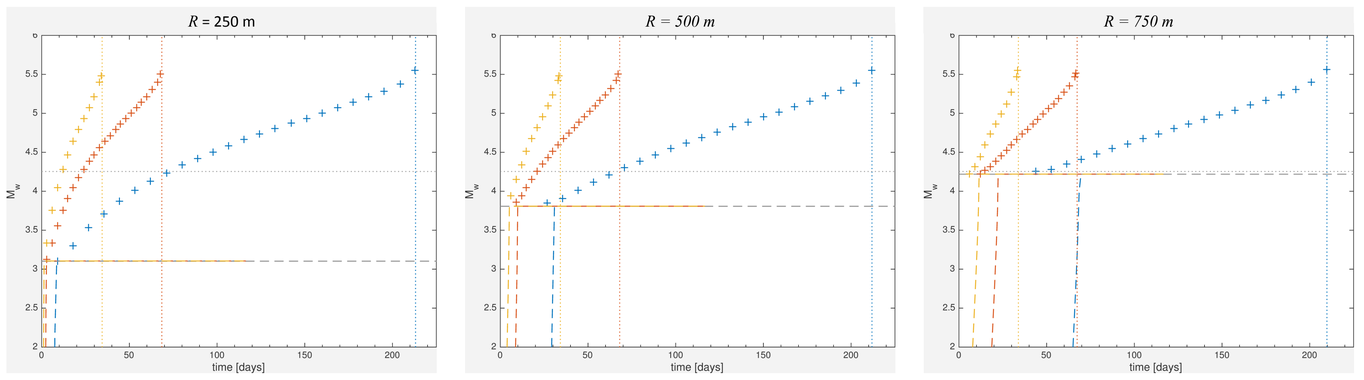

Comparison of maximum M_w for configuration C

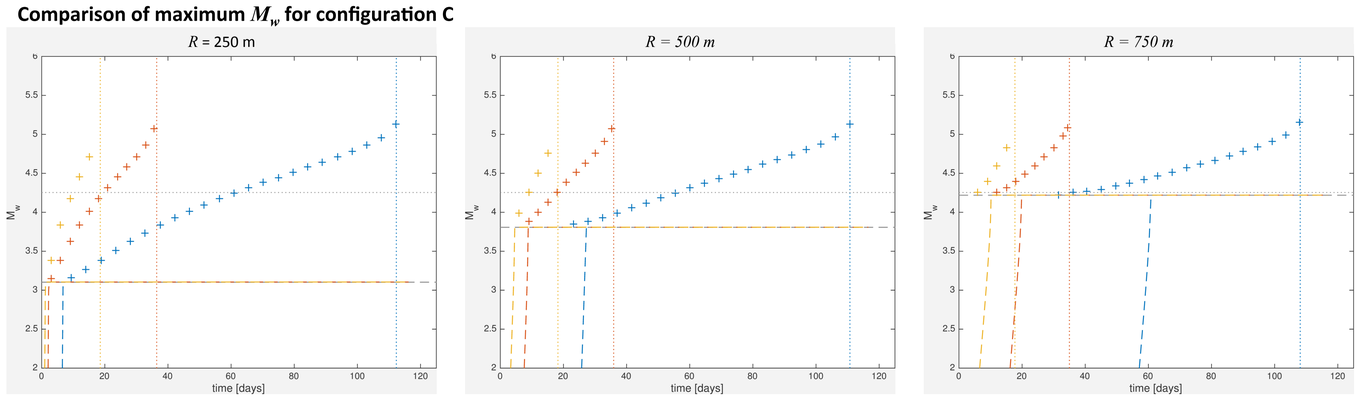

5 PRELIMINARY CONCLUSIONS

M_w of the largest stopping rupture depends on frictional parameters of a fault and only marginally on flow rate and dimension of a reservoir.

Runaway ruptures are less realistic for small than for large reservoirs. Pressure in the reservoir strongly depends on the dimension of reservoir, leading to very high pressures in small reservoirs (up to 550MPa in our case).

Strength parameter S is not a representative parameter because magnitude of stresses are important in this scenario, as supported by the fact that two cases with identical S but different static and initial tractions behaves differently.

REFERENCES

Deichmann, Giardini, 2009. Seismological Research Letters 80(5)
Dyer, Schanz, Ladner, Haring, Spillman, 2008. The Leading Edge 27
Galis, Pelties, Kristek, Moczo, Ampuero, Mai, 2015. *Geophys. J. Int.* 200
Häring, Schanz, Ladner, Dyer, 2008. Geothermics 37(5)
Kammer, Radiguet, Ampuero, Molinari, 2015. *Tribol. Lett.* 57:23
Mai and Beroza, 2000. *Bull. Seism. Soc. Am.* 90
Rubinstein, Cohen, Fineberg, 2007. *Phys. Rev. Lett.* 98
Uenishi, K., 2009. In *Proceedings of the 38th Symposium on Rock Mechanics*

ACKNOWLEDGEMENTS

Research reported in this publication was supported by the King Abdullah University of Science and Technology (KAUST).